A Novel Approach to Extract Water Body from ASAR Dual-Polarized Data

Jianwei Ma[1, 2], Xiaoning Song[1*], Xiaotao Li[2], Pei Leng[1], Fangcheng Zhou[1] and Shuang Li[1]

[1] College of Resources and Environment, University of Chinese Academy of Sciences, Beijing, China

[2] China Institute of Water Resources and Hydropower Research, Beijing, China

[*] Corresponding author, e-mail: songxn@ucas.ac.cn

Abstract. SAR (Synthetic Aperture Radar) has become a useful and efficient method for monitoring flood extent due to its capability of 24-hour and all weather observation. In this paper, a novel approach is proposed to extract water bodies from ASAR dual-polarized images. Firstly, a new SAR image was created from ASAR Dual-Polarized data using a discrete wavelet transformation (DWT) fusion method. Then, a modified Otsu threshold method was used to extract water bodies of Poyang Lake with the new fused image. Next, this image was compared with the one extracted from ETM+ data. The result showed that the fused image was feasible and more accurate. Besides, it could reduce the influences of shadow and noise. Moreover, the approach could be conducted automatically, which is very important under urgent condition for flood monitoring.

1. Introduction

It is important to extract water extent quickly and accurately in early warning and flood monitoring. SAR (Synthetic Aperture Radar) has become a useful and efficient method on monitoring the water extent for its capability of 24–hour and all weather observation [1-2]. The water possesses various backscattering characteristics in terms of different polarized SAR data. How to use multi–polarized SAR data to extract water extent is a hot and difficult issue in flood monitoring. Furthermore, threshold's automatic determination for SAR data has not been effectively solved according to the previous studies.

The remainder of this paper is organized as follows. Section 1 introduces the study area and data sources involved in our method. Section 2 describes the DWT and modified Otsu threshold method in detail. Section 3 mainly discusses the water body extracted from fused ASAR dual-polarized data. Section 4 concludes the paper.

1.1. Study Area

This study focuses on the west extent of Poyang Lake in the lower Yangtze River basin of China (28°25′–29°45′N, 115°48′–116°44′E; Figure 1). The surface water area varies from more than 4000 km^2 during summer monsoon rain season to less than 1000 km^2 in winter [3]. The lake exchanges water with Yangtze River through 40 km long water channel in the northern part, and it plays an important role to weaken flood peaks by storing discharges from five tributaries [4].

1.2. Data

The ENVISAT-1 satellite was launched by ESA (European Space Agency) on March 1st, 2002. The ASAR (Advanced Synthetic Aperture Radar) instrument is a multi-mode sensor which operates at C-band (5.33 GHz) at several polarizations (HH, VV, HV and VH), incidence angles (15°-45°), spatial and radiometric resolutions depending on the functioning mode. The ASAR instrument may operate as a conventional strip map SAR(Image and Wave modes) or as a ScanSAR (Global Monitoring, Wide Swath and Alternating Polarization modes) [5]. At this frequency, atmospheric perturbations can be considered negligible [6].

ASAR has a spatial resolution of approximately 30 m×30 m when operated in the AP mode with HH/VV, HH/HV and VV/VH polarization. In this paper, HH/VV polarized image in AP mode was used to study the water body extraction method, and the data was acquired on July 28, 2004.

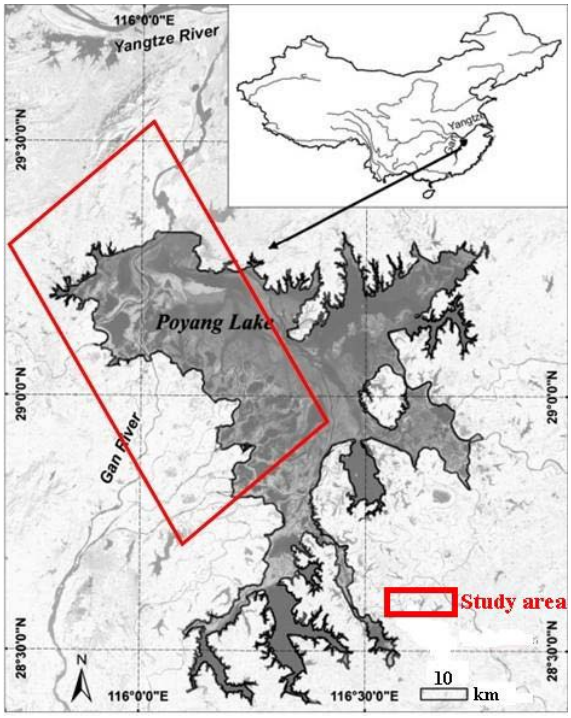

Figure 1. The study area of Poyang Lake, Jiangxi Province, China[3]

2. Method

2.1. Discrete wavelet transformation (DWT)

Discrete wavelet transformation is a mathematical tool developed in the field of signal processing. It can decompose a digital image into a set of multi-resolution images and for two successive resolution levels, each level contains different spatial and digital information. [7]. All fusion techniques have the same flow that the transformed images are combined in the transformation domain using a defined fusion rule, and then are transformed back to the spatial domain to give the fused image. Wavelet transform fusion is more formally defined that it considers the wavelet transforms ω of the two input images $I_1(x,y)$ and $I_2(x,y)$ together with the fusion rule ϕ ,and then the inverse wavelet transform ω^{-1} is computed, the fused image $I(x,y)$ is finally reconstructed :

$$\mathrm{I}(\mathrm{x},\mathrm{y}) = \omega^{-1}\left(\phi\left(\omega(I_1(x,y)),\omega(I_2(x,y))\right)\right) \quad (1)$$

In the case of wavelet transform fusion, all respective wavelet coefficients from the input images were combined using the fusion rule ϕ. Wavelet coefficients with large absolute value contain more

information about the salient features of the images such as edges and lines. So, a good fusion rule needs to take the maximum of the absolute values of the corresponding wavelet coefficients. Besides, weight average scheme [8] or window based on verification scheme [9] is also suggested as a kind of fusion rule.

In this study, daubechies-7 wavelet was chosen as wavelet basis and the number of decomposition levels is 5. Schematic flowchart of DWT between ASAR-AP data is shown in Figure 2.

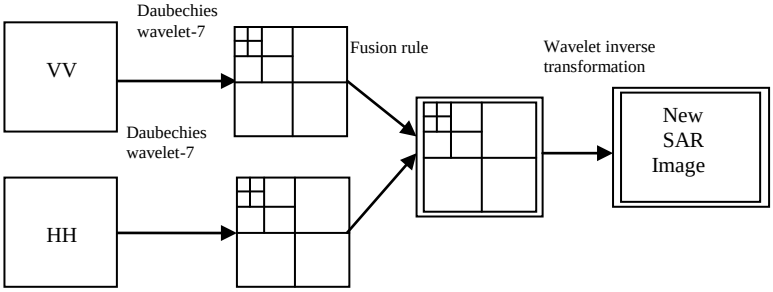

Figure 2. Schematic flowchart of DWT image fusion between ASAR AP data

2.2. Modified Otsu threshold method

In image segmentation, threshold method becomes an effective tool to separate the object from the background when the gray levels are substantially different between them [10]. Otsu method [11] has gained more attention among lots of methods in recent years [12-13]. Otsu method automatically finds the threshold and differentiates targets from background using the histogram of a grayscale image, based on the idea of maximizing the between-class variance [14].

Suppose that the pixels in a given image are represented in l gray levels (0, 1, . . . , l-1). Let n_i denotes the number of pixels at level i, and N denotes the total number of pixels $N=\sum_{i=0}^{l-1} n_i$ .The probability of occurrence of level i is given by $p_i = n_i / N_i$ .Let an image be divided into two classes C_0 and C_1 by threshold t. C_0 consists of pixels with levels{0,1,2, …, t}and C_1 consists of pixels with levels{ t+1,t+2,…,l-1}.Let $p_0(t)$ and $p_1(t)$ denote the cumulative probabilities, $u_0(t)$ and $u_1(t)$ denote the mean levels, respectively. These values are given by:

$$p_i = n_i / N_i \ (p_i \geq 0, \sum_{i=0}^{l-1} p_i = 1) \tag{2}$$

$$p_0(t) = \sum_{i=0}^{t} p_i, \quad p_1(t) = \sum_{i=t+1}^{l-1} p_i \tag{3}$$

$$u_0(t) = \sum_{i=0}^{t} i p_i / p_0(t), \quad u_1(t) = \sum_{i=t+1}^{l-1} i p_i / p_1(t) \tag{4}$$

Let u and $\sigma^2(t)$ represent the mean level of the image and the between-class variance, respectively:

$$u = \sum_{i=0}^{l-1} i p_i = p_0(t)u_0(t) + p_1(t)u_1(t) \tag{5}$$

$$\sigma^2(t) = p_0(t)[u_0(t)\text{-}u]^2 + p_1(t)[u_1(t)\text{-}u]^2 \tag{6}$$

The threshold decided by maximizing the between-class variance proposed in Otsu is:

$$t^* = \arg \max_{0<t<l-1} \left[\sigma^2(t) \right] \tag{7}$$

A Modified method derived from Otsu algorithm was put forward, which combined interclass distance with intra-class distance [15]. $\bar{\sigma}_0^2(t)$ and $\bar{\sigma}_1^2(t)$ denote the variances of the classes C_0 and C_1, respectively:

$$\bar{\sigma}_0^2(t) = \frac{1}{p_0(t)} \sum_{i=0}^{t} (i\ u_1(t))^2 p_i \tag{8}$$

$$\bar{\sigma}_1^2(t) = \frac{1}{p_1(t)} \sum_{i=t+1}^{l-1} (i\ u_1(t))^2 p_i \tag{9}$$

The modified method was as follows, which was proved better than Otsu threshold algorithm [16].

$$t_{new}^{*} = \arg \max_{0<t<l-1} \left[\frac{\sigma^2(t)}{\bar{\sigma}_0^2(t) + \bar{\sigma}_1^2(t)} \right] \tag{10}$$

3. Result

With the proposed method, water body of Poyang Lake was finally extracted using the fused data, which has been described in Figure 5.

3.1. Comparing fused data with single-polarized data in visual inspection and histogram

Figure 3 illustrates the backscattering data of the study area. Visual inspection reveals that the fused data with DWT (Figure 3c) has the maximum contrast, and water borderline is enhanced greatly. In addition, HH polarized data (Figure 3a) is better than VV polarized data (Figure 3b). Figure 4 shows the histogram of each data. It is clear that fused data dealt with DWT has the biggest double-peak, while HH and VV data have smaller ones. This implies that water body will be identified easier with fused data rather than HH data and VV data, and HH performs better than VV. It can also be noticed that the fused data histogram is higher than the others, implying a possibly better identification of classifying.

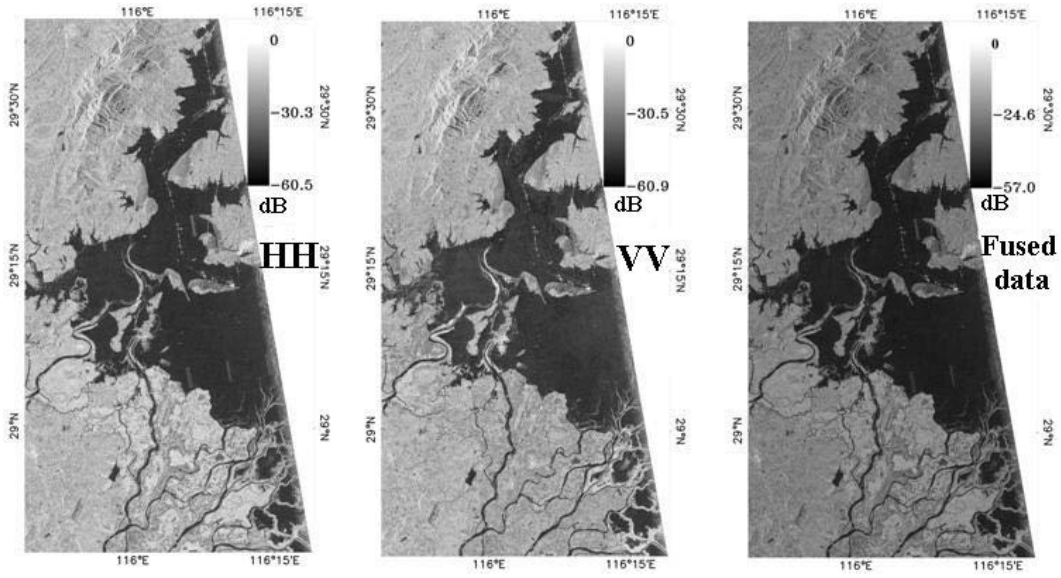

(a)HH data (b) VV data (c) Fused data by DWT

Figure 3. Data of study area

3.2. Comparing fused data with single-polarized data in extracted water body

Water extent was extracted by the proposed modified Otsu algorithm. Part of shadow was classified as water in each image (Figure 5 a, b and c). Obviously, VV shows the most shadow, followed by HH and fused data. The result shows that the method can reduce some influence from shadow, which is suitable for mountain area. In addition, the local picture of the water extent shows that DWT can reduce the noise of the SAR image, which is beneficial for water body extraction. It also can be seen

that VV polarized image has more noise than HH polarized image, which indicates that HH polarized image is a better choice than VV polarized image.

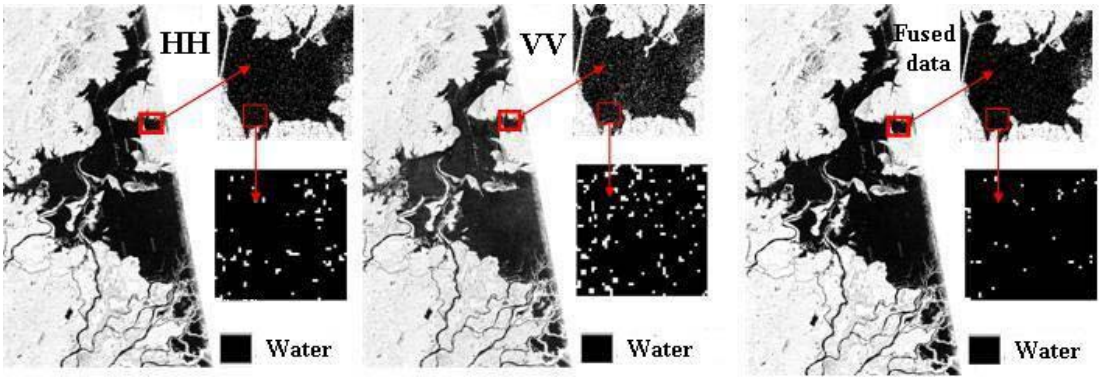

(a) Water body extracted by HH data (b) Water body extracted by VV data (c) Water body extracted by fused data

Figure 5. Comparison of water body extraction

3.3. Accuracy analysis

In order to validate the accuracy of the approach presented in this paper, ETM+ image (acquired on June 30, 2004) in the same area was used to evaluate the result. It was the closest space-borne image to provide a reliable basis for the comparison [17]. The difference of the imaging time between ASAR and ETM+ data would not have much influence on the comparison because there was no rainfall during this period. The results are finally compared with the water extent obtained from ETM+ data.

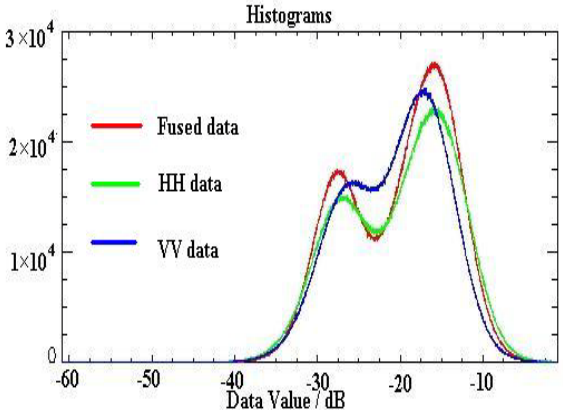

Figure 4. Histogram of fused data, HH data, VV data

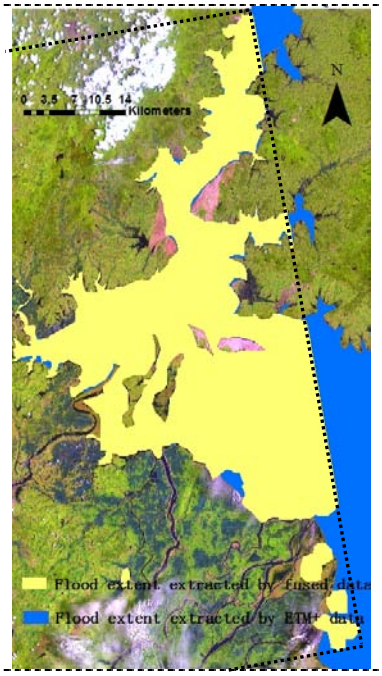

Figure 6. Water extent extracted comparison between fused data and ETM+ data

A best consistency is observed between maps derived from the optical sensor and the fused data. Result shows that more than 97.0% pixels are matched between the water extent extracted by the fused and ETM+ data, while matching percentages got by HH and VV data are about 93.2% and 87.6%, respectively. As Figure 6 shows, the water extent extracted by fused data matches well with the extent

extracted by ETM+ data. It proves that our approach has a higher accuracy, and is suitable to extract water extent during the flood season while the optical remotely sensed data are not available.

4. Conclusions

In this paper, a new method was proposed to extract water extent from ASAR dual-polarized data. Fusing with ASAR dual-polarized data can improve accuracy of extracting water extent compared with single-polarized data because the digital spatial information is improved by DWT fusion method. Moreover, it is capable of reducing some shadow influence so that the method could be applied to mountain area. However, high spatial resolution DEM is needed to reduce shadow completely. It is also capable of reducing radar noise to some extent, which makes positive influence to the result. In addition, the accuracy of threshold is improved by the modified Otsu threshold method, which is of great benefit for the extraction of water extent.

Compared with traditional methods, such as single polarized SAR method, ratio method, muti-temporal method, the method proposed in this paper is more effective because it can be conducted automatically, which is very important during the period of flood.

The proposed method is appropriate on C-band SAR while it is uncertain for other band SAR(S-band, L-band, X-band, et al). Further studies will focus on different backscattering characteristics in different SAR, and to develop a general method extracting water extent on all bands SAR. Besides, comparison among different fusion methods and threshold methods is also our ongoing work.

Acknowledgment

This work is supported by the National Natural Science Foundation of China (Grant No. 41271379) and Special Fund of China Institute of Water Resources and Hydropower Research (Project ID 1120).The ASAR data used in this study was provided by Center for Earth observation and Digital Earth, Chinese Academy of Sciences (http://ids.ceode.ac.cn/), and the ETM+ data was provided by International Scientific Data Service Platform (http://datamirror.csdb.cn/).

References

[1] Badji M and Dautrebande S 1997 *Hydrological Process* **11**(10) 1441-50
[2] Matgen P, Montanari M, Hostache R, et al 2010 *Hydrology and Earth System Sciences* **14** 1773–85
[3] Dronova I, Gong P, Wang L 2011 *Remote Sensing of Environment* **115** 1–17
[4] Zhao X, Stein A, Chen X L, Feng L 2011 *Procedia Environmental Sciences* **3** 105–10
[5] ENVISATASAR product handbook 2004 European Space Agency
[6] Ulaby F T, Fung A K, Moore R K 1981 *Microwave and remote sensing active and passive* (Boston: Artech House)
[7] Zhang Y 2002 *International Archives of Photogrammetry and Remote Sensing* **34**(4) 301–314
[8] Burt P J, and Kolczynski R J 1993 *Proceedings of the 4th International Conference on Computer Vision* 173–182
[9] Li H, Manjunath B S, and Mitra S K 1995 *Graphical Models and Image Processing* **57** 235–45
[10] Kwon S H, 2004 *Pattern Recognition Letters* **25** 1045–50
[11] Otsu N 1979, *IEEE Transactions on Systems, Man, and Cybernetics* **9** 62–66
[12] Rosenfeld A and Torre P 1983 *IEEE Transactions on Systems, Man, and Cybernetics* **13** 231–35
[13] Sauvola J and Pietaksinen M 2000 *Pattern Recognition* **225** 33-36
[14] Mizushima A, and Lu R F 2013 *Computers and Electronics in Agriculture* **94** 29–37
[15] Cai M Y, Wu Q X, S J C 2007 Electronics *Optics and Control* **14**(6) 118–151
[16] Li J G, Huang S F, Li J R 2010 *Journal of Natural Disasters* **19**(3) 139–145
[17] Henry J B, Chastanet P, Fellah K and Desnos L Y, 2006 *International Journal of Remote Sensing* **27** (10) 1920–29